

Development of the Next Generation of Multi-chroic Antenna-Coupled Transition Edge Sensor Detectors for CMB Polarimetry

B. Westbrook¹ · A. Cukierman¹ · A. Lee¹ ·
A. Suzuki¹ · C. Raum¹ · W. Holzapfel¹

Received: 30 September 2015 / Accepted: 16 January 2016 / Published online: 1 February 2016
© Springer Science+Business Media New York 2016

Abstract We present the development of the next generation of multi-chroic sinusoidal antenna-coupled transition edge sensor (TES) bolometers optimized for precision measurements of polarization of the cosmic microwave background (CMB) and cosmic foreground. These devices employ a polarization sensitive broadband self-complementary sinusoidal antenna to feed on-chip band defining filters before delivering the power to load resistors coupled to a TES on a released bolometer island. This technology was originally developed by UC Berkeley and will be deployed by POLARBEAR-2 and SPT-3G in the next year and half. In addition, it is a candidate detector for the LiteBIRD mission which will make all sky CMB and cosmic foreground polarization observations from a satellite platform in the early 2020's. This work focuses on expanding both the bandwidth and band count per pixel of this technology in order to meet the needs of future CMB missions. This work demonstrates that these devices are well suited for observations between 20 and 380 GHz. This proceeding describes the design, fabrication, and the characterization of three new pixel types: a low-frequency triplexing pixel (LFTP) with bands centered on 40, 60, and 90 GHz, a high-frequency triplexing pixel (HFTP) with bands centered on 220, 280, and 350 GHz, and a mid-frequency tetraplexing pixel with bands (MFTP) centered on 90, 150, 220, and 280 GHz. The average fractional bandwidth of these pixel designs was 36.7, 34.5, and 31.4% respectively. In addition we found that the polarization modulation efficiency of each band was between 1 and 3% which is consistent with the polarization efficiency of the wire grid used to take the measurement. Finally, we find that the beams have $\sim 1\%$ ellipticity for each pixel type. The thermal properties of the bolometers were tuned for characterization in our lab so we

✉ B. Westbrook
bwestbrook@berkeley.edu

¹ Department of Physics, University of California, Berkeley, Berkeley, CA 94702, USA

do not report on G and noise values as they would be unsuitable for modern CMB experiments.

Keywords CMB · Bolometers · TES · B-modes · Polarization · Inflation

1 Introduction

In recent years, study of the polarization of the CMB has been at the forefront of experimental cosmology. Searches for B-mode polarization to probe the inflationary epoch and the growth of structures have led to tremendous advances in instrument sensitivity [1–5].

Recent data from the BICEP2/Keck and Planck collaboration suggests that robust characterization of the cosmic foreground at frequencies above and below the peak of the CMB intensity at 150 GHz is required to measure the faint B-mode signature [6]. Figure 1(left) plots the amplitude of BB-polarization from synchrotron radiation, thermal dust, and the CMB (assuming $r = 0.05$) at $\ell \approx 80$ in the BICEP2/Keck field. Since the amplitude of both foregrounds are comparable to or larger than CMB from 30 to 350 GHz, there remains the need to characterize the polarized emission over that frequency range. Figure 1(right) demonstrates that the pixels developed in this work are well suited for this task as the seven bands in the plot provide coverage across this entire frequency range. These pixels are being explored as candidate pixels for the LiteBIRD satellite mission.

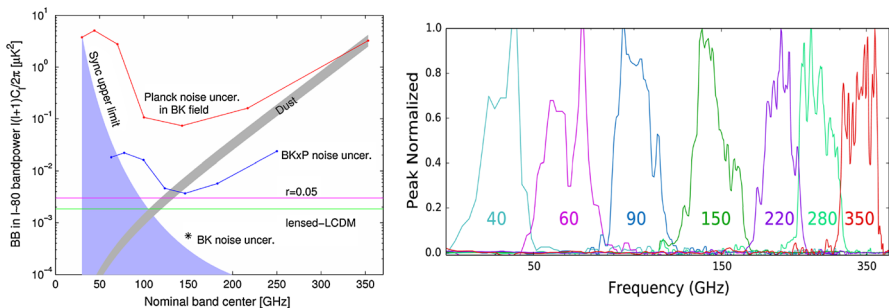


Fig. 1 Left Figure from the BICEP2/Keck and plank collaboration joint analysis demonstrating the need to improve polarization measurements for frequencies surrounding the peak intensity of the CMB [6]. The plot shows the relevant BB-polarization amplitudes of the cosmic foreground and CMB for $\ell \sim 80$ in the BICEP2/KECK field. At frequencies below ~ 100 GHz, contributions to BB polarization from synchrotron radiation are greater than the expected BB signal power from lensed- Λ CDM (green) and $r=0.05$ (magenta) in CMB units. Above ~ 120 GHz, the amplitude of BB power coming from dust in the galactic foreground is also greater than the expected BB signal power from the CMB. Right A plot showing all of the new bands measured in this work, which demonstrates the flexibility of this technology for CMB and foreground polarization studies (Color figure online)

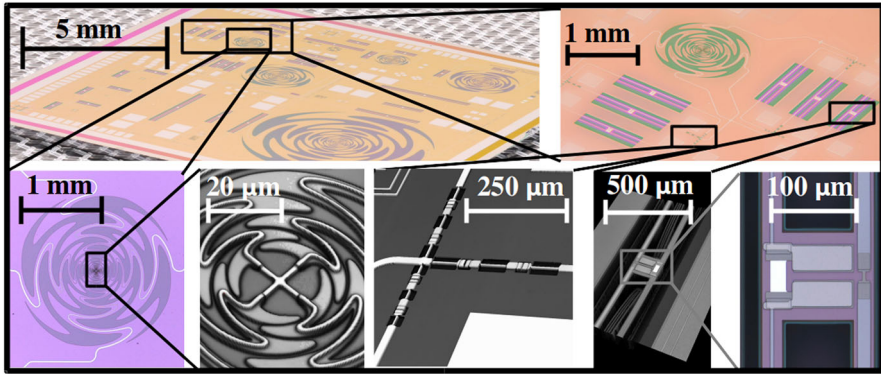


Fig. 2 A series of photographs illustrating the design of these devices. Radiation couples to the sinuous slots in the antenna, which allow a single antenna to receive a large bandwidth of radiation (*bottom left*). The power is delivered to a bank of lumped element filters by a niobium transmission line which separates the incoming radiation into bands (*bottom middle*). The power from each band is then terminated on a Titanium resistor and converted to heat and coupled to a comparatively large palladium block (*bottom second from right*). The temperature fluctuations are monitored by a TES under constant voltage bias (*bottom right*). Another advantage of this design is that the thermal properties of the bolometer can be tuned independently from the optical properties due to the physical separation of the elements on the wafer (Color figure online)

2 Design

The pixel design in this work was originally developed by Roger O' Brient and Aritoki Suzuki and was adapted and expanded by Ari Cukierman and Benjamin Westbrook [3, 7]. The design consists of a broadband self-similar sinuous slots in antenna coupled to two orthogonal superconducting Niobium (Nb) micro-strips. The Nb micro-strip then feeds 3–4 lumped element filters with a common node, which separates the broadband radiation into the pixel's bands as illustrated in Fig. 2. Lumped elements are made by converting the transmission line into coplanar wave guide to increase its impedance over short distance, effectively making it a lumped inductor [8]. Short breaks in the transmission line create tunable capacitive elements to form 3-pole Chebyshev filters. After the radiation is separated into bands, the power for each band is terminated on a normal titanium (Ti) resistor which dissipates the power as heat. This termination resistor is strongly coupled to a large palladium (Pd) block which acts as a thermal ballast for the bolometer island. This Pd element is coupled to an aluminum–manganese (AlMn) transition edge sensor (TES) which converts variations in optical power into current variations through the TES, which are then amplified by a superconducting quantum interference device (SQUID). The Ti termination resistor, the Pd thermal ballast, AlMn TES, and Nb micro-strips, and voltage bias lines are then suspended on an H-shaped, thermally isolated bolometer island as shown in Fig. 2.

For a given frequency range of interest, the size of the antenna and the lumped element filters must be tuned accordingly. In this work, we designed three pixels: a low-frequency triplexing pixel (LFTP) with bands centered on 40, 60, and 90 GHz; a mid-frequency tetraplexing pixel (MFTP) with bands centered on 90, 150, 220, and 280 GHz; and a high-frequency triplexing pixel (HFTP) with bands centered on 220,

280, and 350 GHz. Figure 2 shows a photograph of the test chip containing these three multi-chroic pixels, which were fabricated on a single wafer. It highlights the most important features of these devices for the HFTP.

3 Fabrication

The devices discussed in this proceeding were fabricated at the Marvell Nanofabrication Facility (MNF) at UC Berkeley following a similar process as the production of POLARBEAR-2 detectors [3]. The fabrication steps and parameters are summarized in Table 1. In the table below, all patterning steps include a lithography step completed using Fuji Film OCG 825 35CS photo-resist exposed to patterns printed by a GCA 8500 Wafer stepper system. In addition, each patterning step requires a robust cleaning process to clear away the photo-resist from the previously lithographed layer to prepare the wafer for the next step.

3.1 Wafer Prep

Fabrication begins by coating a 6'' silicon wafer with ~ 40 nm of silicon oxide and ~ 500 nm low stress silicon nitride (LSSN) grown in a low pressure chemical

Table 1 A summary of the fabrication steps used to fabricate these devices

| Step name | Process type | Tool | Approx thickness | Feature size |
|--|---------------------------------------|-----------|------------------|--------------|
| Sacrificial SiO ₂ coating | LPCVD | Tystar 4 | 40 nm | N/A |
| LSSN coating | LPCVD | Tystar 17 | 500 nm | N/A |
| Nb ground plane dep | DC sputtering | Gartek | 300 nm | N/A |
| Nb ground plane patterning | Cl ₂ RIE | Lam7 | 30 nm | 1.2 μm |
| SiO _x microstrep dep | PECVD | Oxford2 | 500 nm | N/A |
| SiO _x microstrep patterning | RIE | Lam6 | 500 nm | 10 μm |
| Nb microstrep dep | DC sputtering | Gartek | 300 nm | N/A |
| Nb microstrep patterning | BCL ₃ /CL ₂ RIE | Lam7 | 300 nm | 0.9 μm |
| AlMn (TES) dep | RF sputtering | MRC944 | 10 nm | N/A |
| Ti dep | RF sputtering | MRC944 | 50 nm | N/A |
| Ti patterning | SF ₆ RIE | Ptherm | 70 nm | 5 μm |
| AlMn (TES) patterning | Al wet etch | Lab Sink | 10 nm | 15 μm |
| Pd thermal ballast dep | EBE | CHA | 500 nm | N/A |
| Pd thermal ballast patterning | Lift off | Lab Sink | N/A | 10 μm |
| LSSN patterning | CF ₄ RIE | Ptherm | 500 nm | 10 μm |
| Wafer dicing | Si WaferSaw | DA4250 | 675 mm | 70 μm |
| Bolometer release | XeF ₂ dry etch | Xetch | 30 μm | 60 μm |
| Wafer PR ash | O ₂ RIE | Xetch | 30 μm | 60 μm |

Note that 4 extra steps are required to construct a micro-strip cross over for dual polarization devices. These steps include two oxide layers, a Nb sputter etch, and a Nb layer

Keys: *LPCVD* low-pressure chemical vapour deposition, *RIE* reactive ion etching, *PECVD* plasma enhanced chemical vapor deposition, *EBE* E-beam evaporation

vapor deposition (LPCVD) furnace, which will support the released bolometer structure.

3.2 RF Circuit and Antenna

A self-similar sinuous antenna slot, the lumped element inductor and capacitor features, and holes for releasing the bolometer are created by patterning a layer of 300 nm thick Nb. A 500 nm thick layer of Silicon Oxide (SiO_x) is then deposited to provide a dielectric material for the micro-strip transmission lines. The micro-strip, RF filters, and TES bias lines are created by deposited and patterning a second layer of Nb.

3.3 TES, Load Resistor and Thermal ballast

A sputter etch removes any native oxide on the niobium strip ensuring that the AlMn TES and Ti resistor do not have any ohmic contact at the operating temperature of these devices. In the same vacuum step, AlMn and Ti are sequentially sputtered onto the wafer. The Ti and AlMn layers are patterned to form the load resistor and TES respectively. After a lithography step the Pd thermal ballast is deposited and patterned via a lift off process.

3.4 Bolometer Patterning and Release

H-shaped slots are created in the LSSN to allow access for dry XeF_2 gas for the bolometer release, which etches away $\sim 30 \mu\text{m}$ of silicon beneath the H-shaped structure. Finally, the photo-resist is removed using an O_2 plasma prior to testing and characterization.

3.5 Process Notes and Comments

The fabrication flow of these pixels benefits greatly from the heritage of the UC Berkeley fabrication efforts for the POLARBEAR2 project and is quite robust. Despite the large number of steps, the process has good intra-wafer uniformity and wafer-to-wafer consistency, which is aided by the fact that each step only requires that tools operate well within their specifications. In addition, the design can be closely monitored throughout the process to ensure that each step is completed as designed and any given wafer will meet the yield and performance requirements of a given experiment similar to the capabilities of the National Institute for Standards and Technology (ACTPol/Advanced ACTPol) and Argonne National Laboratory (STP-3G).

4 Characterization

The characterization of these devices was carried out in a optical test cryostat at the Physics department of the UC Berkeley. Figure 3 right is photograph of the

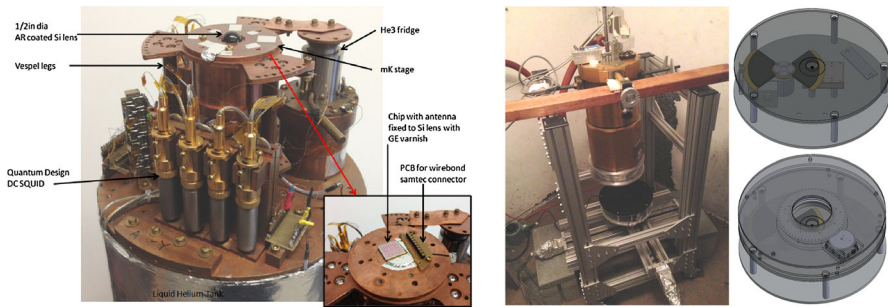


Fig. 3 *Left* A photograph of the cold stage of the cryostat used for this testing illustrating the mounting scheme of the pixel. *Right* A photograph of the cryostat on cart with the beam mapper below. The CAD images on the right show how the optical chopper and LN₂ are configured (Color figure online)

inside of the cryostat and figure it mounted above. Fig. 3 left the beam-mapping set up.

A single die is mounted as shown in Fig. 3(left) for each cryogenic run. A 1/2"-diameter lenslet is anti-reflected coated with molded Welch–Fluorocarbon hemispheres of varying thicknesses. The AR coating is chosen to meet the quarter- λ for a frequency roughly centered on the spectral response of the unfiltered antenna for each pixel type. In this work, three separate dies were cooled with three different lenslets.

The bolometers are cooled to 270 mK using a He3 sorption fridge pre-cooled with pumped liquid helium (LHe). The wafers are then biased with a constant DC voltage on the order of 30–50 μ V and amplified with Quantum Design SQUID readout controller. A stable optical load is created by chopping between either an electric ceramic heater or liquid nitrogen and room temperature at 20–25 Hz.

For spectral measurements, a custom-made Fourier transform spectrometer (FTS) couples the chopped optical signal to the cryostat with a large high-density polyethylene (HDPE) lens, which is designed to fill the beam of the detector full at wavelengths for 2 mm and below. The data are collected as an interferogram and Fourier transformed into a spectral response. Figure 1(left) contains spectral measurements from the bands measured in this work.

Polarization modulation efficiency and beam maps data use liquid nitrogen as the thermal source, which is apodized with a 1/4" Eccosorb aperture. A beam map is taken by translating the chopped source in a grid pattern beneath the window of the cryostat in 1/8" increments while recording the bolometer response at each spatial location. Once the beam map is taken, the source is centered on the peak and rotatable polarizing grid is placed in front of the window. The polarizing grid is then stepped in 5° increments, while the output of the bolometer is recorded to measure the polarization modulation efficiency.

The measurement results for 90-GHz MFTP channel is shown Fig. 4 to visually demonstrate the performance of a single channel on one of the pixels. The remainder of the data from the other channels (including those on the LFTP and HFTP) is summarized in Table 2. These results are consistent with our expectations from simulating these devices in EM simulation software as shown in the left panel of Fig. 4. Since the

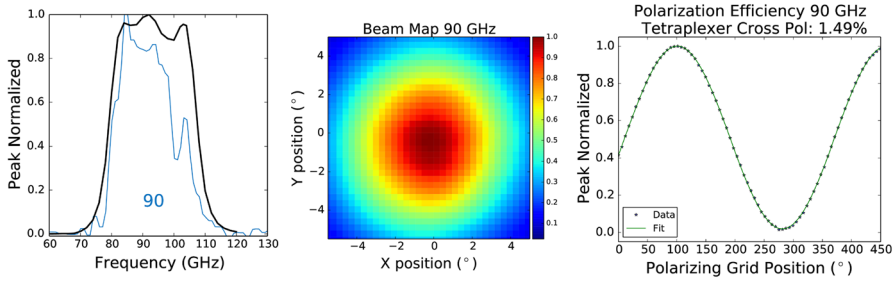


Fig. 4 Measurement results from the 90-GHz MFTP channel. *Left* Spectral response (blue) and simulated expected spectral response (black). *Center* Beam map data. *Right* Polarization modulation efficiency data (black dots) and fit (green lines) (Color figure online)

Table 2 Summary of the optical performances of each of three new pixels types developed in this work demonstrating that these pixels provide the foundation for tailoring this technology to a broad variety of CMB experiments

| Band (GHz) | LFTP | | | MFTP | | | HFTP | | |
|------------|------|-----------|--------|------|-----------|--------|------|-----------|--------|
| | BW % | Pol Eff % | Ell. % | BW % | Pol Eff % | Ell. % | BW % | Pol Eff % | Ell. % |
| 40 | 37.5 | 2.3 | 1.9 | – | – | – | – | – | – |
| 60 | 38.1 | 1.5 | 2.2 | – | – | – | – | – | – |
| 90 | 34.4 | 1.5 | 1.8 | 33.8 | 1.5 | 1.2 | – | – | – |
| 150 | – | – | – | 28.3 | 1.9 | 1.3 | – | – | – |
| 220 | – | – | – | 37.2 | 1.5 | 1.2 | 27.2 | 2.4 | 1.5 |
| 280 | – | – | – | 38.5 | 2.7 | 1.1 | 34.2 | 2.1 | 1.4 |
| 350 | – | – | – | – | – | – | 32.8 | 2.4 | 1.3 |

thermal properties of the bolometer must be tuned on an experiment-by-experiment basis and can be tuned independently from the optical properties, we do not report on these values here.

5 Conclusion

As the field progresses toward understanding CMB and foreground polarization at unprecedented levels so must the technology used to characterize them. These prototype pixels are well tailored to future CMB polarization experiments, most notably LiteBIRD. This work demonstrates the flexibility of this technology as its optical properties are well suited for observations from 20 to 380 GHz.

Acknowledgments The work for this project was carried out with support from NASA Grant NNG06GJ08G.

References

1. T. Matsumura et al., *J. Low Temp. Phys.* **176**, 733 (2014)
2. Planck Collaboration et al., *Astron. Astrophys.* **571**, A22 (2014)
3. A. Suzuki et al., *J. Low Temp. Phys.* **650**, 176 (2014)
4. B. Benson et al., *International Society for Optics and Photonics SPIE* **9153**, 1PB (2014)
5. The Polarbear Collaboration et al., eprint [arXiv:1011.0763](https://arxiv.org/abs/1011.0763) (2010)
6. BICEP2/Keck and Planck Collaborations et al., *Phys. Rev. Lett.* **114**, 101301 (2015)
7. M. Myers et al., *Appl. Phys. Lett.* **86**, 114103 (2005)
8. D.M. Pozar, *Wiley*, 9780471448785 (2004)